Pergamon

Int. J. Heat Mass Transfer. Vol. 40, No. 14, pp. 3387–3394, 1997

Printed in Great Britain
0017–9310/97 $17.00+0.00

PII: S0017–9310(96)00375–4

Double-diffusive convection in a rotating cylinder with heating from below

JINHO LEE
Department of Mechanical Engineering, Yonsei University, Seoul 120-749, Korea

SHIN HYUNG KANG
Department of Mechanical Engineering, Konyang University, Nonsan, Choongnam 320-800, Korea

and

MYUNG TAEK HYUN
Department of Mechanical Engineering, Cheju National University, Cheju-Do 690-756, Korea

(*Received* 26 *April* 1996 *and in final form* 22 *October* 1996)

Abstract—Experimental investigations are made to study the convective phenomena of an initially stratified salt-water solution due to bottom heating in a uniformly rotating cylindrical cavity. Three types of global flow patterns initially appear depending on the effective Rayleigh number (Ra_η) and Taylor number (Ta): stagnant flow regime, single mixed layer flow regime and multiple mixed layer flow regime. The number of layers at its initial stage and the growth height of the mixed layer decreases as Ta increases for the same Ra_η. It is ascertained in the rotating case that the fluctuation of interface between layers is weakened, the growth rate of mixed layer is retarded and the shape of interface is more regular compared to the stationary case. © 1997 Elsevier Science Ltd.

1. INTRODUCTION

Double-diffusive natural convection occurs when simultaneous heat and species transfer with different diffusivity establishes temperature and concentration gradients that determines the density distribution within a fluid. It frequently occurs in oceans, magma chambers, as well as in many engineering applications such as solar ponds, liquid gas storages, transpiration cooling, crystal growth and metal solidification processes.

As pointed out by Ostrach [1], various convection modes can exist, depending on how temperature and concentration gradients are oriented relative to one another. Early double-diffusive works were performed for vertical temperature and concentration gradients to explain some unusual oceanographical phenomena [2]. Later investigations considered initially solute-stratified fluids that are heated (cooled) from vertical enclosure walls [3–9]. The formation, interaction and merging of convective layers were observed due to the significant difference in diffusivities of heat and mass. Recently, double diffusion induced by simultaneously imposed horizontal temperature and concentration differences have been considered [10–13]. Most recently, mechanisms responsible for high-frequency oscillatory double-diffusive convection have been discussed [13–16].

The problem of heating from below on a stratified fluid was initiated with the study on the mechanism of multiple layered flow structures. It was of interest to ascertain the mechanism responsible for the genesis and maintenance of a layered flow structure. In this case, double-diffusive layers may be formed successively from the bottom layer [17–20] and the mixed layer moves upwards by the energy balance of eddies [21]. It was also examined that the secondary layer grew with time and final thickness of all layers were almost equal [22].

The effect of rotation often plays very important role in many transport processes such as oceanic and atmospheric flow and crystal growth. In many practical engineering applications of materials processing, the entire system rotates steadily about a vertical axis [23–26]. In spite of its importance, most probably due to the difficulty of experiment, previous studies were mostly concentrated on stationary systems. The effect of rotation on a salt fingering interface between two mixed layers was experimentally studied [23] and the effect of rotation on the linear stability of an unbounded region of a stratified fluid has been analyzed [25].

In this paper, an attempt is made to study experimentally double diffusion in an initially solute-stratified liquid, housed within a uniformly rotating cylinder with heating from below. Particular attention is made to the flow configurations which give rise to double-diffusive convective motions under the effect of rotation.

NOMENCLATURE

Ar	aspect ratio, H/D
D	diameter of cylinder
g	gravitational acceleration
H	height of cylinder
Le	Lewis number, κ/κ_S
Ra_S	solutal Rayleigh number, $g\,\alpha_S\Delta S\,H^3/\kappa_S\nu$
Ra_T	thermal Rayleigh number, $g\,\alpha_T\Delta T\,H^3/\kappa\nu$
Ra_η	effective Rayleigh number, $g\,\alpha_T\Delta T\,\eta^3/\kappa\nu$
ΔS	concentration difference
Ta	Taylor number, $4\Omega^2H^4/\nu^2$
ΔT	temperature difference
z	axial coordinate.

Greek symbols

α_T	coefficient of thermal expansion
α_S	coefficient of solutal expansion
η	reference height, $-\alpha_T\,\Delta T/\alpha_S\,(dS/dz)$
κ	thermal diffusivity
κ_S	solutal diffusivity
ν	kinematic viscosity
Ω	angular velocity.

2. EXPERIMENTS

The experimental apparatus is schematically shown in Fig. 1. The test section is a vertically standing transparent acrylic cylinder with 10 mm outer wall thickness and 100 mm inner diameter and height. The top and bottom walls of the test section are made of aluminum plates for the constant temperature condition. Two reservoirs are attached to the top and bottom plates to keep it at different, but constant temperatures.

In the test section, two constant temperature baths and a computer are laid on the rotating table. The rotating rate of the table is controlled by an inverter and a power slip ring is installed on a rotating axis for supplying electrical power which is needed for the computer and the A/D converter. The thermocouple is mounted on a carriage which could be moved with a programmable stepping motor, and are connected to a 16 bit A/D converter via a pre-amplifier. This yielded a resolution of 0.5°C. The thermocouple is moved through the solution with a speed of 20 mm/s and data are acquired at 1 kHz. Temperature profiles are obtained at intervals of 5 mm in the vertical direction. Three thermocouples are installed on the top and bottom plates, respectively, to check the non-uniformity of the temperature over the entire plates.

Initially the cylinder is filled with a salt-water solution using the standard step method with 30 steps to establish the desired initial salinity profiles. It took about 2 h to have a linear concentration profile in the test section by diffusion. To avoid mixing of the solution, the bottom wall is heated after the system is spun up. In order to measure concentration, the sam-

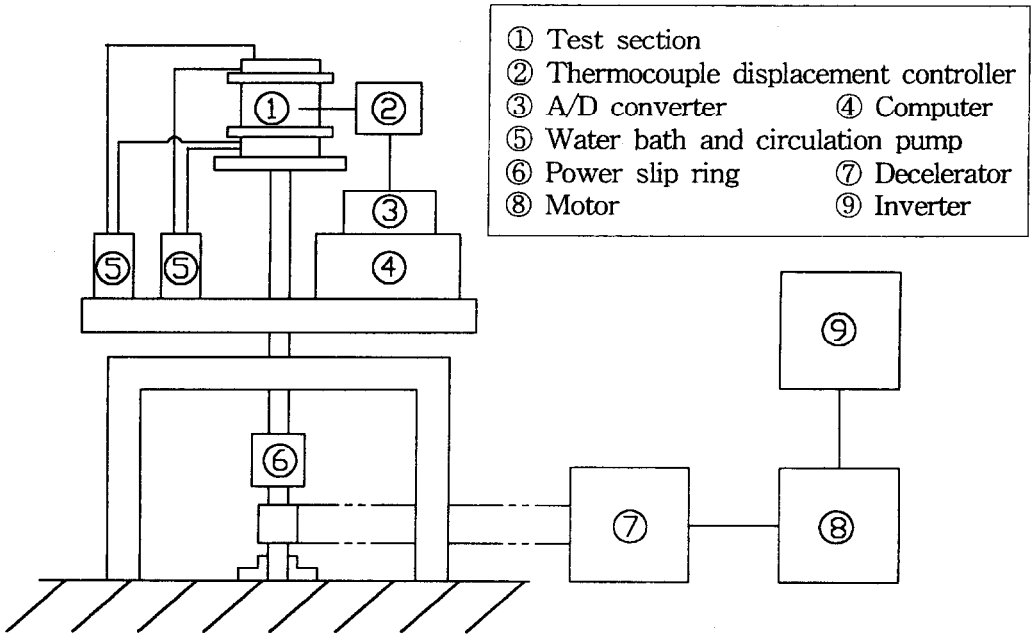

Fig. 1. View of the total experimental apparatus.

ple extraction method is used. A minute amount of solution is extracted through the hole which has been made on the wall at intervals of 5 mm in the vertical direction and its refractive indices are read through a refractometer. This procedure is repeated several times, and the average refractive index is then converted into the concentration by a conversion chart. The deviation of the refractive indices are about $\pm 2\%$.

A shadowgraph technique is used to obtain the development of the initial layer formation. The cavity is illuminated by passing a 10 mW He–Ne laser beam through a spatial filter assembly and the image picture is taken by a camera.

The ranges of the parameters covered in the present experiments are $Le = 100$, $\Delta T = 5.0$–$21.1^{\circ}C$, $\Delta C = 2$–8 wt%, $\Omega = 0$–30 rpm, $Ra_T = 1.48 \times 10^8$–7.27×10^8, $Ra_s = 1.10 \times 10^9$–4.47×10^9, $Ra_\eta = 1.05 \times 10^4$–$6.19 \times 10^7$ and $Ta = 0$–1.82×10^8.

3. RESULTS AND DISCUSSION

3.1. *Stationary case*

For the stationary system three types of global flow patterns are observed according to the effective Rayleigh number (Ra_η), which is based on the reference height η and represents the relative magnitude of solutal stratification to the destabilizing bottom heating [4]; the stagnant flow regime for $Ra_\eta < 1.05 \times 10^4$, the single mixed layer flow regime for $1.91 \times 10^4 < Ra_\eta < 6.66 \times 10^5$ and the multiple mixed layer flow regime for $1.22 \times 10^6 < Ra_\eta$. The local heat flux at the top of the first convection layer may be affected somewhat by the constraint at the top boundary as was shown by Turner *et al.* [2]. The critical value of Ra_η here may thus need more validation against the tank height and top boundary condition.

Figure 2 shows global flow patterns for stationary case with effective Rayleigh numbers. The stagnant flow regime [Fig. 2(a)] is formed when the thermal buoyancy is very weak compared with a given solutal stratification ($Ra_\eta < 1.05 \times 10^4$). There appears no motion at all because the destabilizing thermal effect is not enough to overcome the stable salt stratification. Consequently, the initial concentration distributions remain almost unchanged with time and the temperature profiles are unstably stratified. Compared to the Bénard convection generated by only temperature difference due to bottom heating, the flow occurs at higher temperature difference than in the Bénard convection case due to the additional stable solutal stratification.

As the bottom heating increases ($1.91 \times 10^4 < Ra_\eta < 6.66 \times 10^5$), the stability of the system decreases and the thermal buoyancy becomes sufficient for generating motion. The thermal boundary layer develop above the heated surface with some thickness while the fluid above the convective mixing layer still remains stagnant. This flow regime is called a single mixed layer flow regime [Fig. 2(b)]. The mixing layer expands with time and the interface separating the stable and convecting layer gradually rises up with small oscillations. Finally, the whole cavity is filled with the convectively mixed single layer. In this case, the initial concentration profile remains almost unchanged and the temperature variation is linear due to conduction in the stagnant layer, while the temperature and concentration profiles in the mixed layer become uniform due to vigorous fluid motion. The concentration near the interface between the two layers is widely changed.

When the destabilizing thermal effect becomes high ($1.22 \times 10^6 < Ra_\eta$), a series of mixed layers successively develops; the first one starting from the bottom and others above previously formed layers [Fig. 2(c)]. The formation of the first mixed layer is the same as in the case of the single mixed layer flow regime. Since heat diffuses more rapidly than salt through the top of the layer, thermal boundary layer is generated in the lower part of the stagnant region. The irregular motion occurs at the bottom of stagnant region making the second mixing layer and a new convecting layer starts above it. As the flow progresses, the second convective layer merges into

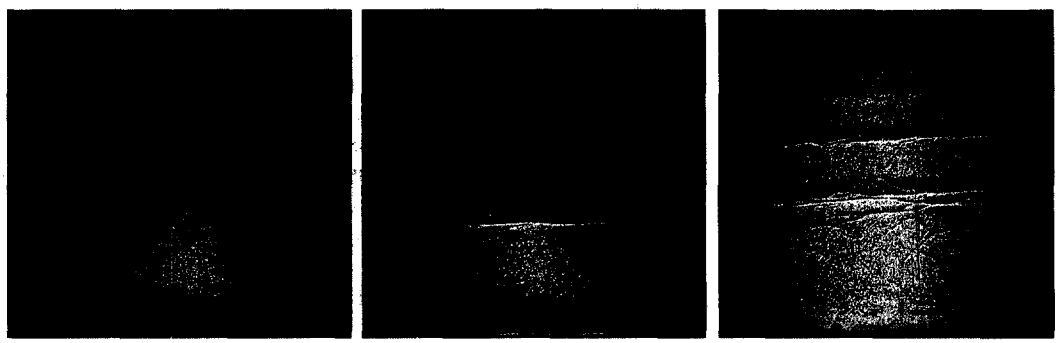

(a) (b) (c)

Fig. 2. Global flow patterns for stationary case with Ra_η at $t = 60$ min: (a) stagnant flow regime ($Ra_\eta = 1.05 \times 10^4$), (b) single mixed layer flow regime ($Ra_\eta = 6.66 \times 10^5$), and (c) multiple mixed layer flow regime ($Ra_\eta = 8.14 \times 10^6$).

the first mixing layer because the concentration difference between the two layers becomes small and the second layer loses its thermal buoyancy energy faster than that of the first one. After continuous formation and merging of layers, only a single mixed layer exists at the final stage. In this way an initially linear distribution of salinity is well mixed and a convecting layer nearly uniform in temperature is produced. Note that the present temperature profiles here is uniform in each layer while it appears S-shaped in the case of side wall heating [3–9]. It is observed that greater temperature differences at the bottom cause more layers to appear.

3.2. *Rotating case*

In the rotating system, three rotating rates (10, 20, 30 rpm) are examined to see the effect of rotation in an initially stratified double-diffusive fluid heating from below. The evolution of flow patterns are similar to those of the stationary case, but the number of initial mixing layers, their growth rates and the range of Ra_η classifying the type of layer formations are different.

Figure 3 shows the classification of three different flow regimes at the initial stage according to Ra_η and Ta. We may ascertain that the flow regimes shift to higher Ra_η as the rotating effect becomes strong. In the case of stagnant flow regime (small destabilizing thermal buoyancy compared with stabilizing initial solutal buoyancy) the temperature distributions are unstably stratified whereas the concentration profiles do not change, because the thermal buoyancy cannot overcome the initial solutal buoyancy. It can be observed in Fig. 3 that the ranges of stagnant flow regimes are $Ra_\eta < 1.05 \times 10^4$ for $Ta = 0$, $Ra_\eta < 4.45 \times 10^4$ for $Ta = 2.02 \times 10^7$, $Ra_\eta < 6.73 \times 10^4$ for $Ta = 8.07 \times 10^7$ and $Ra_\eta < 1.30 \times 10^5$ for $Ta = 1.82 \times 10^8$, respectively.

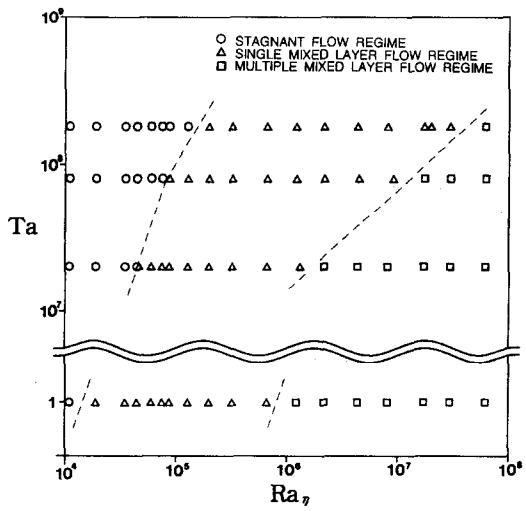

Fig. 3. Flow patterns depending on Ra_η and Ta.

Figure 4 represents shadowgraph of single mixed layer for various Taylor numbers at an early stage of the experiment ($t = 7$ min). Irregular flows caused by an increasing thermal buoyancy force generates mixed layers as mentioned in the stationary case. However, the strength of flow is weakened as rotating rates increase because the flow in an axial direction is inhibited by the rotating effect. As shown in Fig. 4, the fluctuation of interface wanes and the growth rate of the mixed layer is retarded with increasing rotation of the system. The ranges of single mixed layer flow regimes are $1.91 \times 10^4 < Ra_\eta < 6.66 \times 10^5$ at $Ta = 0$, $4.66 \times 10^4 < Ra_\eta < 1.22 \times 10^6$ for $Ta = 2.02 \times 10^7$, $7.51 \times 10^4 < Ra_\eta < 9.10 \times 10^6$ for $Ta = 8.07 \times 10^7$ and $1.99 \times 10^5 < Ra_\eta < 2.97 \times 10^7$ for $Ta = 1.82 \times 10^8$, respectively. Figure 5 represents a typical vertical temperature and concentration profiles for single mixed layer flow regime at the core of cavity. Due to vigorous fluid motion in convecting layer, the temperature and concentration distributions become uniform. In the stagnant region, the linear temperature profiles reveal diffusion dominating mode of heat transfer and the initial concentration profiles remain almost unchanged. As the experiment progresses, the interface between the two regions moves upwards with time.

Shadowgraphs of mixed layer formation which have the same effective Rayleigh number, but different Taylor numbers, are shown in Fig. 6. We can see that the number of layers in the rotating case decreases as Taylor number increases for the same effective Rayleigh number at the initial stage (Fig. 6 at $t = 40$ min). There exist multi-layers at an early stage [Fig. 6(a) and (b) at $t = 40$ min]. The occurrence and development mechanism of the multiple mixed layer in the rotating cavity is the same as that in the stationary case. This phenomena occurs as the thermal boundary layer developing near the bottom becomes unstable and generates irregular flows due to heat transfer through the bottom of the cavity as the bottom temperature difference increases. This flow causes the interface to highly contort and irregularly fluctuate. The irregular fluctuation of interface engulfs a small amount of fluid in the stagnant region into a mixed layer while making the concentration difference near the interface smaller and then fluids of the stagnant region near the interface mixes with that of the mixed layer [21].

Through this process, the mixed layer gradually expands and the second layer appears above the first layer due to fast diffusion of heat through the interface. This mechanism reduces and eventually causes the decay of stagnant region. The reduction of concentration difference between two convecting layers causes the strength of the flow to weaken in each layer and it eventually makes two layers merge into one. The shape of the interface is nearly flat and the fluctuation almost disappears at that time and the newly formed single layer expands very slowly [Fig. 6(a) and (b) at $t = 220$ min]. When Taylor number is 1.82×10^8 with the same effective Rayleigh number, the single mixed

(a) Ta=0 (b) Ta=2.02x10^7 (c) Ta=8.07x10^7

Fig. 4. Shadowgraphs of single mixed layer flow with Ta at $t = 7$ min: $Ra_\eta = 8.14 \times 10^6$.

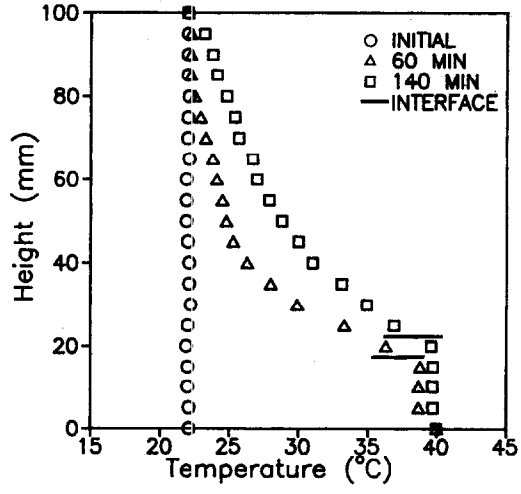

(a) Temperature profiles

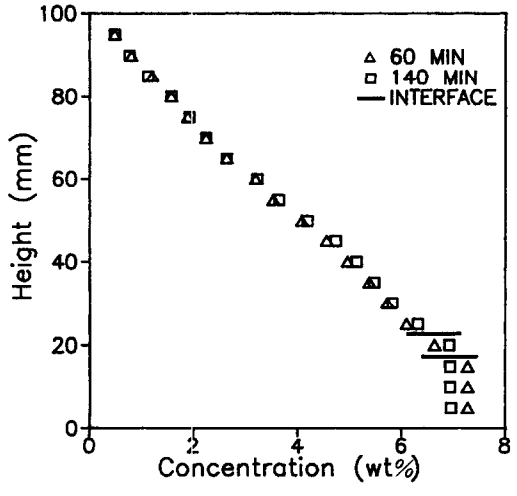

(b) Concentration profiles

Fig. 5. Vertical temperature and concentration profiles at the core for single mixed layer flow regime: $Ra_\eta = 6.66 \times 10^5$, and $Ta = 2.02 \times 10^7$.

layer flow is directly formed [Fig. 6(c)]. As the rotating rate increases, the relative importance of the rotation should be important and this leads to the weakening of the convective activity, driven by the bottom heating. In consequence, multiple mixed layer flow regime can be observed in higher Ra_η as the rotating effect becomes strong. The regions of multiple mixed layers are observed at $Ra_\eta > 1.22 \times 10^6$ for $Ta = 0$, $Ra_\eta > 1.32 \times 10^6$ for $Ta = 2.01 \times 10^7$, $Ra_\eta > 1.73 \times 10^7$ for $Ta = 8.07 \times 10^7$ and $Ra_\eta > 6.19 \times 10^7$ for $Ta = 1.82 \times 10^7$, respectively. The interface's inclination in the temperature and concentration profile was not observed in the experiment though we carefully checked it. However, it was observed in our ongoing experiment which is in the case of lateral heating in a solute-stratified fluids. In such an experiment, it became steeper as the rotating speed increases.

Figure 7 represents a typical vertical temperature and concentration profiles at the core of cavity for multiple mixed layer flow regime. The temperature and concentration distributions in the mixed layer are uniform by convective mixing. In the stagnant region, temperature distributions become unstably stratified while the concentration profiles are maintained with initially stratified distributions like other cases. At the interface, concentration varies rapidly and temperature varies smoothly owing to the difference of diffusivities of salt and heat. Two layers, initially formed, are merged into one at about 200 min.

Figure 8 represents the growth height of mixed layer with time in a single mixed layer flow regime. As shown in Fig. 8(a), the height of mixed layer is increased when Ra_η becomes large. The interface of initial mixed layer moves up quickly within 50 min and then grows slowly thereafter. Since the temperature gradient is suddenly imposed at the bottom of the cavity, the irregular fluctuation of the interface at the early stage is induced (Fig. 6 at $t = 40$ min). As much time has passed, the shape of the interface is nearly flat and the development of mixed layer becomes very slow because a mixed layer is developed by diffusion of

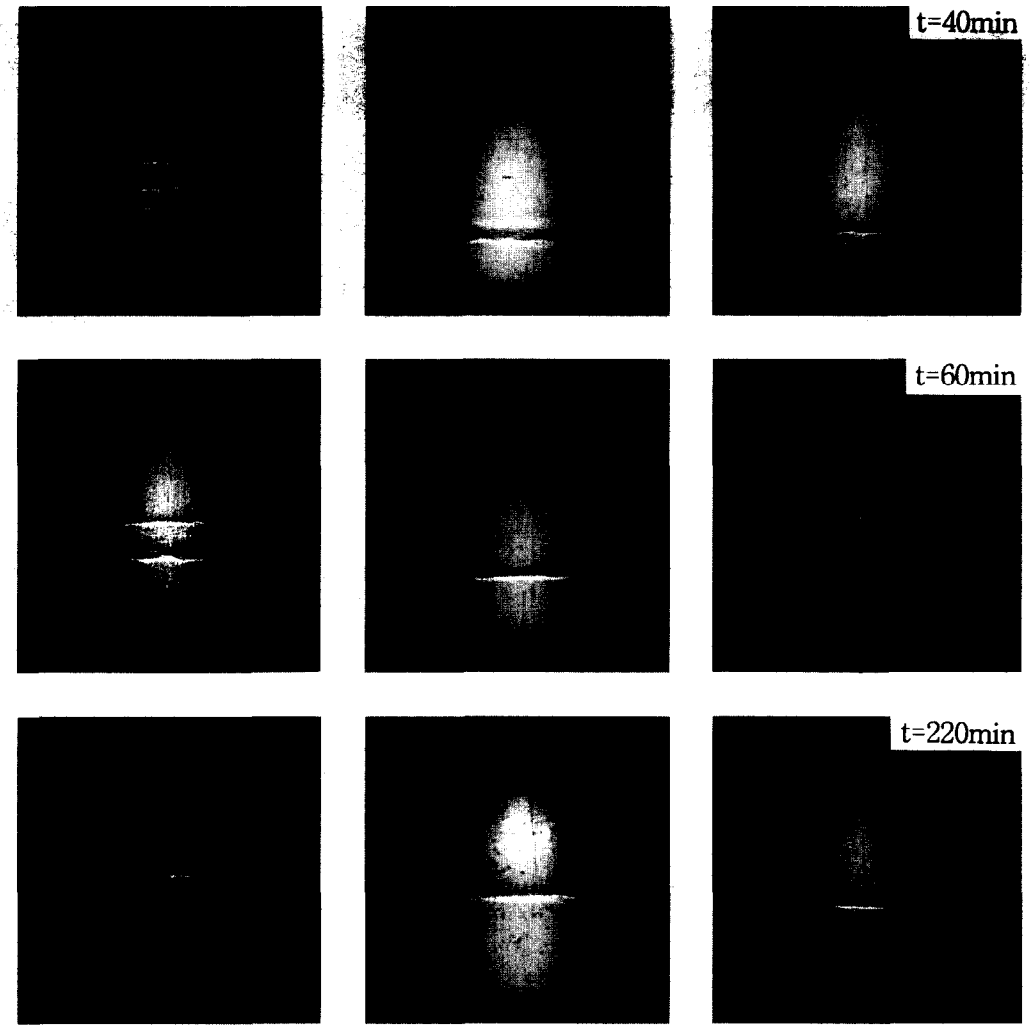

Fig. 6. Shadowgraphs of multiple mixed layer flow with Ta and time.

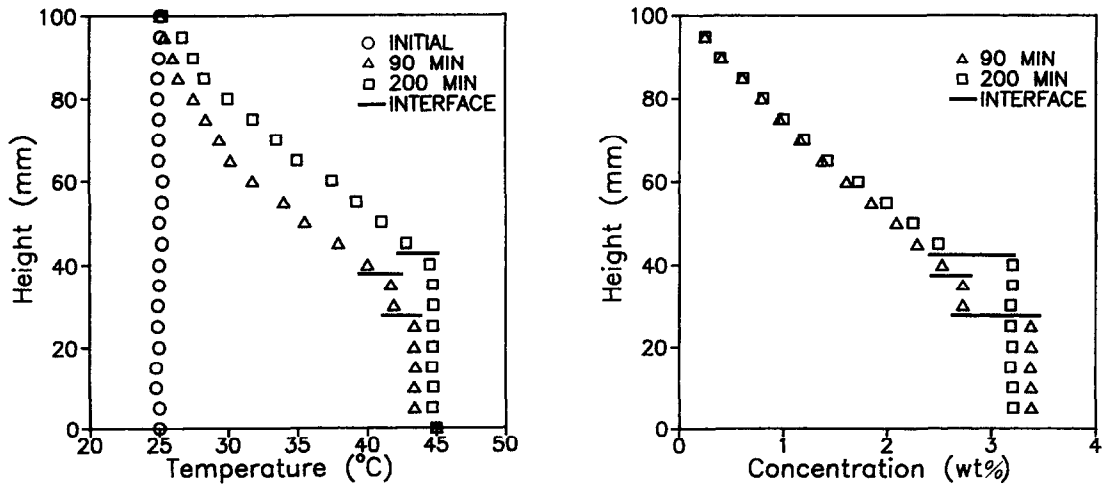

Fig. 7. Vertical temperature and concentration profiles at the core for multiple mixed layer flow regime: $Ra_\eta = 9.10 \times 10^5$, and $Ta = 2.02 \times 10^7$.

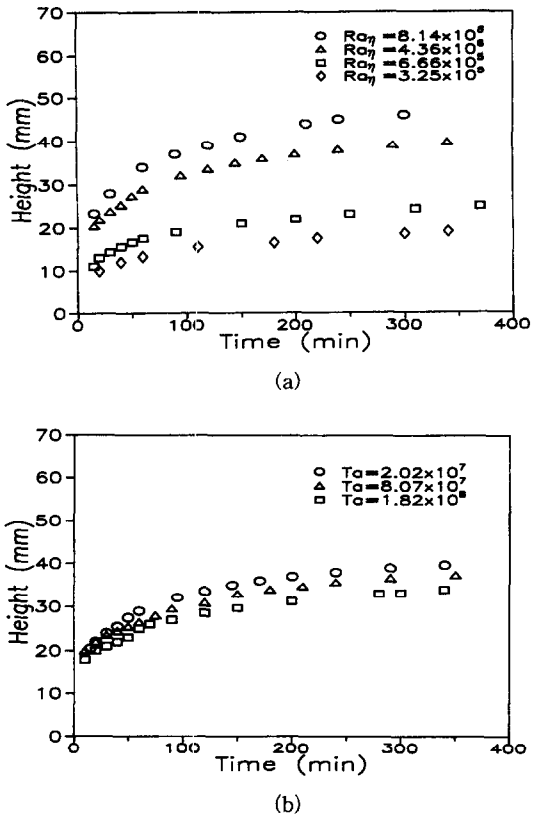

Fig. 8. Height of single mixed layer with time: (a) $Ta = 2.02 \times 10^7$, and (b) $Ra_\eta = 4.36 \times 10^5$.

concentration through the interface (Fig. 6 at $t = 60$ min). Figure 8(b) shows the growth rate of convecting layer according to variation of Taylor numbers for $Ra_\eta = 6.19 \times 10^7$. As the Taylor number is increased (rotating effect becomes strong), the height of mixed layer is reduced as mentioned before.

4. CONCLUDING REMARKS

This paper represents the evolution of the double diffusive convection of an initially stratified salt-water solution within a rotating cylindrical cavity of aspect ratio 1.0 due to heating from below. The type of initially formed flow pattern is classified into three cases depending on the effective Rayleigh number and Taylor number: stagnant flow regime, single mixed layer flow regime and multiple mixed layer flow regime. When the rotating rate increases the relative influence of the rotation becomes so important that the convective activity, induced by heating from below, weakens. In consequence, the number of layers in the rotating case is less than that of the stationary case for the same effective Rayleigh number and the thickness of the mixing layer decreases with increasing rotation. The temperature and concentration profiles are both uniform in each convecting layer due to vigorous fluid convective motion and they are linear for the stagnant region in the case of rotating as well as in the stationary cases.

REFERENCES

1. Ostrach, S., Natural convection with combined driving forces. *PhysicoChemical Hydrodynamics*, 1980, **1**, 233–247.
2. Turner, J. S., *Buoyancy Effects in Fluids*, Chap. 8. Cambridge University Press, Cambridge, 1973.
3. Thorpe, S. A., Hutt, P. K. and Soulsby, R., The effect of horizontal gradients on thermohaline convection. *Journal of Fluid Mechanics*, 1969, **38**, 375–400.
4. Chen, C. F., Briggs, D. G. and Wirtz, R. A., Stability of thermal convection in a salinity gradient due to lateral heating. *International Journal of Heat and Mass Transfer*, 1971, **14**, 57–65.
5. Huppert, H. E., Kerr, R. C. and Hallworth, M. A., Heating or cooling a stable compositional gradient from the side. *International Journal of Heat and Mass Transfer*, 1984, **27**, 1395–1401.
6. Bergman, T. L. and Ungan, A., A note on lateral heating in a double-diffusive system. *Journal of Fluid Mechanics*, 1988, **194**, 175–186.
7. Lee, J., Hyun, M. T. and Moh, J. H., Numerical experiments on natural convection in a stably stratified fluid due to side-wall heating. *Numerical Heat Transfer*, 1990, **18**, 343–355.
8. Kamakura, K. and Ozoe, H., Numerical analysis of transient formation and degradation process of multilayered roll cells with double-diffusive natural convection in an enclosure. *Numerical Heat Transfer*, 1993, **23**, 61–77.
9. Hyun, M. T. and Bergman, T. L., Direct simulation of double-diffusive layered convection. *Journal of Heat Transfer*, 1995, **117**, 334–337.
10. Lee, J. and Hyun, M. T., Experiments on thermosolutal convection in a shallow rectangular enclosure. *Experimental Thermal Fluid Science*, 1988, **1**, 259–265.
11. Hyun, J. M. and Lee, J. W., Double-diffusive convection in a rectangle with cooperating gradients of temperature and concentration. *International Journal of Heat and Mass Transfer*, 1990, **33**, 1605–1617.
12. Han, H. and Kuehn, T. H., Double-diffusive natural convection in a vertical rectangular enclosure—I. Experimental study. *International Journal of Heat and Mass Transfer*, 1991, **34**, 449–459.
13. Jiang, H. D., Ostrach, S. and Kamotani, Y., Unsteady thermosolutal transport phenomena due to opposed buoyancy forces in shallow enclosures. *Journal of Heat Transfer*, 1991, **113**, 135–140.
14. Beckermann, C., Fan, C. and Mihailovic, J., Numerical simulations of double-diffusive convection in a Hele-Shaw cell. *International Video Journal of Engineering Research*, 1991, **1**, 71–82.
15. Alavyoon, F., Masuda, Y. and Kimura, S., On natural convection in vertical porous enclosures due to opposing fluxes of heat and mass prescribed at the vertical walls. *International Journal of Heat and Mass Transfer*, 1994, **37**, 195–206.
16. Hyun, M. T., Kuo, D. C., Bergman, T. L. and Ball, K. S., Direct simulation of double diffusion in low Prandtl number liquids. *Numerical Heat Transfer*, 1995, **27**, 639–650.
17. Shirtcliffe, T. G. L., Transport of the diffusive interface in double-diffusive convection with similar diffusivity. *Journal of Fluid Mechanics*, 1973, **57**, 27–43.
18. Huppert, H. E. and Linden, P. F., On heating a salinity gradient from below. *Journal of Fluid Mechanics*, 1979, **95**, 431–464.

19. Lewis, W. T., Incropera, F. P. and Viskanta, R., Interferometeric study of mixing layer development in a laboratory simulation of solar pond conditions. *Solar Energy*, 1982, **28,** 389–401.
20. Bergman, T. L., Incropera, F. P. and Viskanta, R., Interaction of external and double-diffusive convection in linearly salt-stratified systems. *Experimental Fluids*, 1987, **5,** 49–58.
21. Harindra, Fernando, J. S., The formation of a layered structure when a stable salinity gradient is heated from below. *Journal of Fluid Mechanics*, 1987, **182,** 525–541.
22. Tanny, J., Kerpel, J. and Tsinober, A., On the layered structure in a stable solutal gradient heated from below. *Experimental Fluids*, 1989, **8,** 161–164.
23. Schmitt, R. W. and Lambert, R. B., The effects of rotation on salt fingers. *Journal of Fluid Mechanics*, 1979, **90,** 449–463.
24. Ostrach, S., Fluid mechanics in crystal growth—the 1982 Freeman Scholar Lecture. *Journal of Fluids Engineering*, 1983, **105,** 5–20.
25. Kerr, O. S. and Holyer, J. Y., The effect of rotation double-diffusive interleaving. *Journal of Fluid Mechanics*, 1986, **162,** 23–33.
26. Sung, H. J., Cho, W. K. and Hyun, J. M., Double-diffusive convection in a rotating annulus with horizontal temperature and vertical solutal gradients. *International Journal of Heat and Mass Transfer*, 1993, **36,** 3773–3782.